Geochemical Studies of Rare Earth Elements (REE) in Ion Adsorption Clays (IAC) in Gua Musang, Kelantan

Nur Afikah Fendy[1], *Roniza* Ismail[1*], *Nor Shahida* Shafiee[1] and *Abdul Hafidz* Yusoff [2]

[1]Department of Geoscience, Faculty of Earth Science, Universiti Malaysia Kelantan, Jeli, Malaysia
[2]Faculty of Bioengineering and Technology, Universiti Malaysia Kelantan, Jeli, Kelantan, Malaysia

Abstract. Rare earth element (REE) become the 'critical metals' for green technology development that have been rapidly expanded worldwide in these days. REE is mainly originated from granitic rocks. REE in ion adsorption clay (IAC) is the product from weathering of granite. IAC are believed to store high concentration of heavy rare earth element (HREE) and light rare earth element (LREE). Gua Musang is selected for this study because it is located on the three longitudinal belts that composed of acid volcanic igneous rocks from Main Range, Senting and Boundary Range Granites. In this study, the characteristics of ion adsorption clays and REE distribution in Gua Musang have been studied by mineralogy and geochemical analyses. Rocks and soil samples were collected closed to the granite bodies and its surrounding to represent its weathering products. Polarised optical microscopy was used for petrography and mineralogy studies. From fieldwork observation, Gua Musang lithologies composed of carbonate facies, argillaceous facies and pyroclastic facies. X-Ray Fluorescence (XRF), X- Ray Diffraction (XRD) and Inductive Coupled Plasma Microspectrometry (ICP-MS) were used accordingly to characterise the composition of major and trace elements in IAC samples. REE value in Pulai are the highest concentration as iron nodule have been found in the sampling area. Sample from Boundary Range granite also reported store high concentration of REEs in this study.

1 Introduction

Rare earth element (REE) is the group of seventeen chemical elements that occur together in the periodic table. The group consists of scandium (Sc), yttrium (Y) and the 15 lanthanide series elements. It is divided as light rare earth (LREE) (from lanthanum to gadolinium) and heavy rare earth (HREE) (from terbium to lutetium). REE is quite abundant exist together with most of the minerals found in the earth crust. Because these metals have so many similar qualities, they are frequently discovered together in geologic deposits [1]. In this century, the rare earth element is used in wide range application especially high-tech products such as

* Corresponding author: roniza@umk.edu.my

cellular telephones, computer hard drives, electric and hybrid vehicles, flat-screen monitors and televisions.

China become the major supplier of REE in the world and have been mined in large scale for the lateritic or ion absorption clay deposits. This is because the REE in this deposit type is claimed to be easily extracted with dilute acid and alkali. This is because the REE in this deposit type is claimed to be easily extracted with dilute acid and alkali. According to the Centre for Strategic and International Studies (CSIS), China produces more than 85% of the world's rare earths and holds two-thirds of the worldwide supply of rare metals [2]. According to [1,3] the majority of the world's heavy Rare Earth Elements (REE) come from regolith-hosted IAC which is centred in Southern China that found in weathered crusts of igneous bedrock, predominantly granitic. This deposit type contains high concentration of heavy rare earth element (HREE) and released less radioactive waste.

In IAC's, REE are believed to be weakly adsorbed into clay minerals dominantly kaolinite and halloysite [3]. The mechanism starting with, Rare Earth Elements (REEs) bearing minerals abundant in certain igneous rocks generally granite breakdown to REE^{3+} during chemical weathering, then absorb on the surface of weathered rock forming minerals (clay) and produce ion-adsorption clay REE deposits in high-temperature and tropical regions [4]. Ion adsorption ores are believed to accumulate on the saprolite zone (accumulation zone) of soil profile.

This work is focussing on the distribution of rare earth element (REE) of IAC in Gua Musang, Kelantan. This state is selected because Gua Musang has various granitic pluton. Geochemical method is conducted in this research to determine the chemical characteristics along with petrography studies. The major element is needed in identifying and validating the mineral's existence and was analysed using X-Ray Diffraction (XRD) and X-Ray Diffraction Fluorescence (XRF). Petrography analysis are important to determine the relationship between mineral association and REE distribution in ion adsorption deposit. Inductively Coupled Plasma Mass Spectrometry (ICP-MS) was used in order to determine the REE concentration in the soil samples.

2 Geological Setting

According to [5], Peninsular Malaysia is divided into three longitudinal belts, Western Belt, Central Belt and Eastern Belt. Each belt has its own distinctive characteristics and geological development. As mentioned in [6], the granitoids in Malaysia, Thailand and Myanmar share some petrological and geochronological which permits them to classified into the belts. Kelantan is one of the unique states which located on those three belts [6].

Lithologies in Gua Musang divided into few facies which are carbonate facies, argillaceous facies, volcanic and pyroclastic facies. Some part of Gua Musang also composed of granite which come from Main Range Granite, Senting Granite and Boundary Range as shown in Fig. 1 below. Main Range Granite refer to intrusive in western peninsular belt and separated with central belt granite by Bentong-Raub Suture line. Main Range Granite is dominated on the western part of Gua Musang stretching along western of the state boundary of Perak and Pahang [7] while Boundary Range is distributed on the east part of Gua Musang. Boundary range is a batholith that dominated by felsic granitic and granodiorite to basic diorite and gabbro [8].

3 Methodology

3.1 Mapping and Sampling

Mapping and sampling were conducted around selected area (in South-East area) of Gua Musang, Kelantan. Target sampling is based on the preliminary study on the literature review and geological study of the study area. Geological map from Mineral and Geoscience Department Malaysia (JMG) (Fig.1) is used to aid in the selection of the sampling area. Granite and nearest area are targeted for sampling. The soil samples (approximately 500g-1000g) are collected in the saprolite horizon of the soil profile. Rock samples are collected based on granite distribution for petrography and mineralogy study. The sampling details is shown in Table 1.

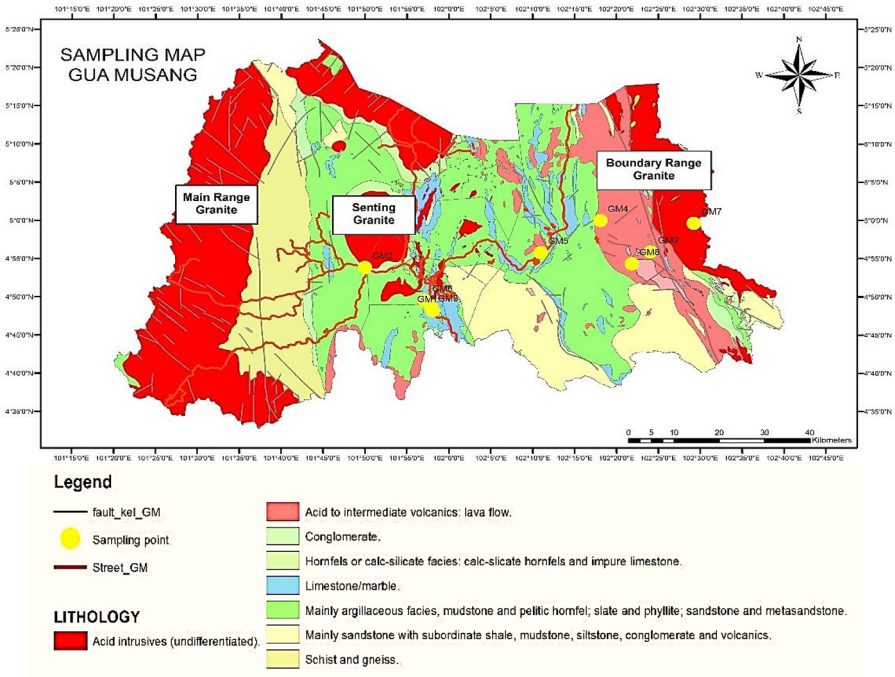

Fig. 1. Geological and Sampling Map of Gua Musang.

Table 1 Sampling Details

Station	Location	Formation	Sample
GM1	Tanah Putih	Telong	Soil
GM2	Kuala Betis	Senting Granite	Soil
GM3	Pulai	Nilam Marble	Soil
GM4	Paloh	Aring	Soil
GM5	Ciku	Telong	Soil
GM6	Pulai	Telong	Soil

Station	Location	Formation	Sample
GM7	Aring	Boundary Range granite	Soil
GM8	Aring	Aring	Soil
GM9	Paloh	Aring	Soil
GM10	Bandar Gua Musang	Senting Granite	Rock
GM11	Subong	Nilam Marble	Rock

3.2 Mineralogy and Petrographic analysis

Rock samples were sent to Universiti Kebangsaan Malaysia (UKM) laboratory for thin section preparation in order to proceed for mineralogy and petrography purposes.

Petrography description is important to correlate it with the results from chemical analyses. Optical polarised microscopy was used to investigate the mineral distribution and morphological evaluation of the samples.

3.3 Chemical analyses

Major elements and mineral identification were determined using X-Ray Fluorescence (XRF) and X- Ray Diffraction (XRD) (Bruker Benchtop XDR D2 Phaser) respectively. It is important to see the variation in element composition for each sample especially for mineral identification and correlation. Four samples (GM1, GM2, GM3 and GM5) were sent for XRD analysis and five samples (GM1, GM2, GM3, GM5 and GM6) were sent for XRF analysis. Inductive Coupled Plasma Microspectrometry (ICP-MS) is used to measure concentration of REE in the sample. Sample GM4, GM5, GM6, GM7, GM8 and GM9 were sent for ICP-MS test. Microwave digestion method is used for sample preparation. Station GM8 were selected for soil profile analysis (in cut slope area) to determined REE concentration in soil profile layering. Soil samples in different horizon (in pedolith and saprolite zone) were sampled to identify the accumulation zone of REE.

4 Result and Discussion

4.1 Mineralogy and Petrography Analysis

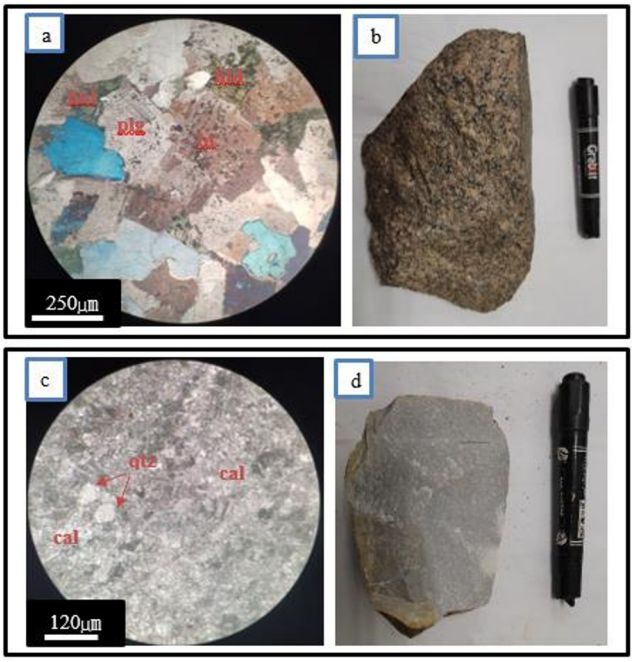

Fig. 2. a) crossed polarized,XPL of petrography study b) granite hand specimen c) crossed polarized,XPL of petrography study d) limestone hand specimen (hbl:hornblend, bt:biotite, qtz:quartz, px:pyroxene, plg:plagioclase, cal:calcite).

Lithology in Gua Musang is mainly composed of carbonate facies, argillaceous facies, volcanic and pyroclastic facies. Some area covered by granite from Main Range granite, Boundary Range granite and Senting granite. Pink granite in Fig. 2 were collected in

Bandar Gua Musang that belong to Senting granite batholith in centre of Gua Musang. This pink granite is composed of plagioclase feldspar which can be identified by albite twining as shown in Fig. 2a. Quartz, biotite and hornblende are amongst the minerals that fill the composition of the sample. GM7 is collected in granite body which belong to Boundary Range granite (in Aring). GM8 and GM9 showed the pyroclastic lithology also have sampled in Paloh which located within Aring Formation.

Fig. 2c represents the petrography of limestone sample in Subong which belongs to Nilam Marble Formation (Permian to Late Triassic) and could be deposited from marine environment [9]. From fieldwork observation, limestone body is distributed on the North-East of Gua Musang and some of the limestone body were exposed and form karst topography (Fig. 3). Petrographic of limestone (Fig. 2a) shows the sample is dominated by calcite mineral which can be identified by its colourless appearance, moderate to low relief and grey extinction colour under XPL. The structure of the sample is non-foliated and the texture is granoblastic based on the irregular and angular grains of the matrix. Sample GM6 also was collected in Nilam Marble Formation which is located near to Senting granite in Pulai.

Fig. 3. Karst topography in North-East Gua Musang, Kelantan

4.2 X-Ray Diffraction (XRD)

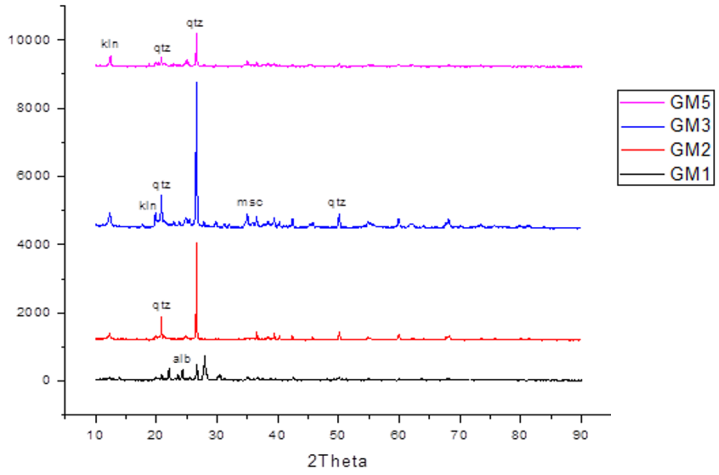

Fig. 4. X-Ray Diffraction (XRD) analysis of soil samples (kln:kaolinite, qtz:quartz, msc:muscovite, alb:albite)

Fig. 4 shows the minerals composition in 4 IAC samples based on XRD analysis. The major minerals in GM1 is albite where the dominant peak can be seen on 23Å and followed by muscovite on 35Å, quartz and kaolinite. According to [10] a study at the nanoscale indicates that albite is a REY (yttrium) carrier, where REY is able to embedded inside the crystal lattice of albite. The samples dominantly composed by feldspar group and kaolinite minerals. Kaolinite and halloysite are the major host for REE in IAC. Sample GM3 has the highest percent of quartz followed by GM2, GM5 and GM1 on the peak 26Å.

4.3 Major Element Analysis

Table 2 shows the major elements of the bulk samples from XRF analysis. The concentration of SiO_2 in the range of 50% to 70%, while Al_2O_3 within 22% to 35 wt%. TiO_2 and CaO are the lowest elements concentration. Sample GM5 contains the fewest percent of SiO_2 and high percent of Al_2O_3. This is because the GM5 sample represent laterite soil. Concentration of Al_2O_3 is elevated in laterite and quite related with deposition of bauxite ore [11]. Concentration of Fe_2O_3 in sample GM6 is the highest (12.27 wt%) due to the existence of iron nodule in the sampling area which can contribute to the higher concentration of Fe_2O_3. The composition of TiO_2 is slightly higher in GM2 and GM6 (1.22 and 1.31 wt% respectively). These two samples were collected in Pulai which is known as a gold deposition area and located within the Gold Central Belt zone [12].

Table 2 Major element composition (wt.%) of IAC soil samples determined by XRF analysis

Samples	Elements composition(wt.%) in oxide					
	SiO_2	Al_2O_3	Fe_2O_3	K_2O	TiO_2	CaO
GM1	69.19	28.20	0.96	1.18	0.07	0.40
GM2	65.13	25.33	6.94	1.23	1.23	0.14
GM3	70.29	22.78	1.89	4.23	0.81	0
GM5	54.57	34.44	7.09	2.93	0.87	0.10
GM6	67.13	18.08	12.34	0.87	1.32	0.26

4.4 REE patterns analysis from ICP-MS Result

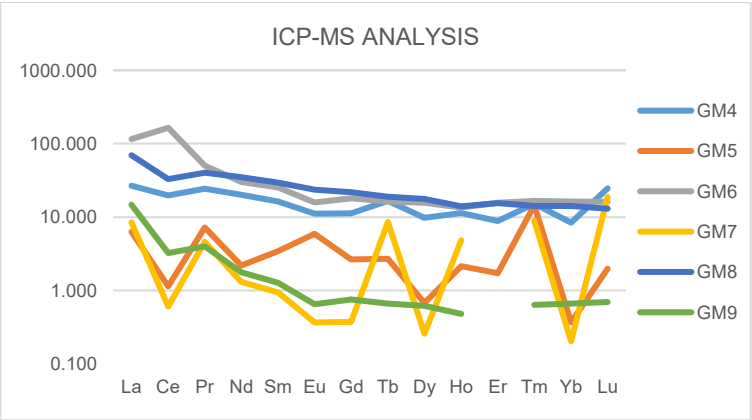

Fig. 5. Normalisation of REE pattern from ICP-MS result

The REE concentration from ICP-MS analysis is presented in Fig. 5 and the normalisation is done based on [13]. From the normalisation patterns it shows that positive Ce anomaly for sample GM6 (Ce/Ce*≥1) as the sample is in laterite soil. The highest total REE concentration in Gua Musang is on GM6, GM8 and followed by GM4. These three samples were collected in three different areas (Pulai-GM6, Aring-GM8, Paloh-GM4). The normalisation trend for these three samples is almost the same. GM6 is the place where the mineralisation of iron nodule has been found in this sampling area. Stated by [14] study shows that iron oxides can be structurally bound with REE by re-mobilization process and high-volatile fluid discharge that can facilitates REE minerals. The lithology in the GM8 area is covered by pyroclastic sediments such as welded tuff and lapilli. These pyroclastic sediments are believing to carry REE from the volcanic activities. From geochemical view, its shows that the concentration on REE in the sample near Senting granite group (GM6) is higher than the sample that collected near Boundary Range granite (GM8) while the concentration of yttrium (Y) shows the highest in station GM6 (43.91ppm). From petrographic analysis shows that GM6 composed of albite mineral (result is not shown in this paper). According to [15] albitization of igneous rocks in nature can be the main factor for the contribution of REE concentration. Samples for GM5, GM7 and GM9 shows the lowest REE concentration.

4.5 Geochemistry of soil profile

Fig. 6 shows soil profile analysis for selected area in Paloh, Gua Musang. This analysis is to show the distribution of REE in soil profile layering. REE enrichment is reported higher in saprolite zone (B-horizon of soil profile) were also known as completely weathered zone [3]. Grain size for these three samples layers are clay size where the gravel particle has nominal diameter ≤2mm. The colour of the soil sample is darker when going down the soil profile (A-horizon:light maroon, B-horizon:dark red, C-horizon:dark brown).

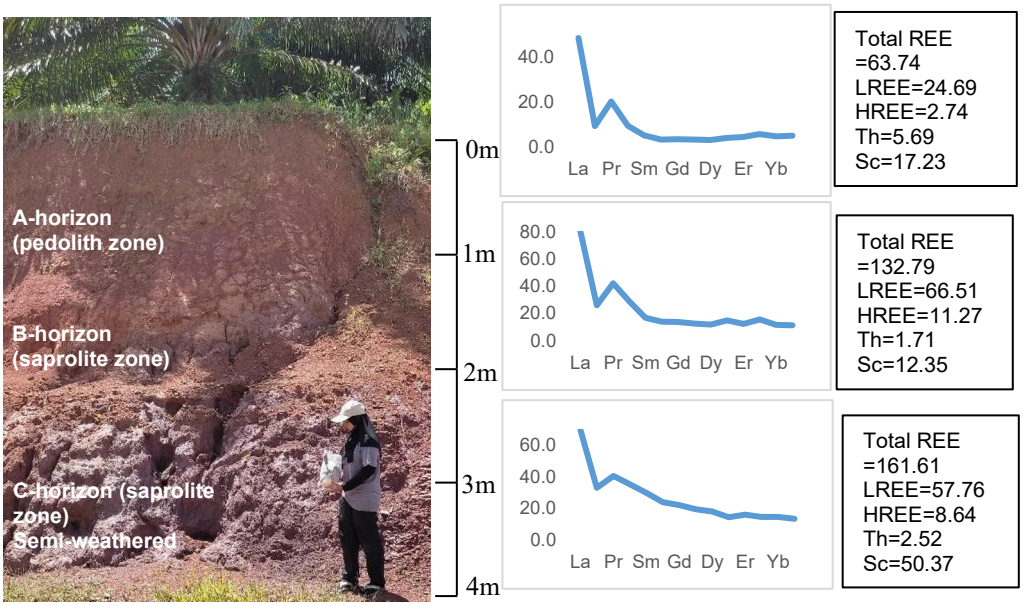

Fig. 6. Soil Profile analysis

In term of REE concentration, normalisation graph pattern and total REE (in ppm) concentration is provided in Figure 6. The pattern shows negative Ce anomaly for all three layers sample where (Ce/Ce*≤1). Depletion of REE concentration happen in pedolith zone

(A-horizon) with total REE concentration is 63.74ppm which is smaller than other horizons. According to [16], REE are frequently depleted in near-surface horizons and accumulate in deeper horizons. From the analysis, saprolite zone (B-horizon) contains total REE 132.79ppm while C-horizon 161.61ppm. B-horizon store high concentration of LREE (66.51ppm) and HREE (11.27ppm) compare to A-horizon and C-horizon. C-horizon is the area where the parent rock began to weathered. This zone called as semi weathered zone as the rock fragments from different sizes were found in this area. This area contains the highest total REE (161.61ppm) because the concentration of Scandium is contributed with 50.37ppm. Based on previous study, [17] brown soil and chernozems can store high concentration of Sc because the parent rock is closed to C-horizon and can contribute to high concentration of Sc.

5 Conclusion

Sample GM6 store the highest concentration of REE (573.89ppm) according to existence of iron nodule. It is supported by XRF result shows the highest concentration of Fe2O3 (12.27wt%). GM8 is the second highest of total REE (400.57ppm) and the sample located from Boundary Range granite. Pyroclastic volcanic rocks in Aring Formation (sample GM4-233.24ppm) adjacent to Boundary Range Granite also store high concentration of total REE among the samples based on pyroclastic lithology. This pyroclastic rock composed of kaolinite mineral. Sampling location in GM4 (Paloh) is lies on the Lebir Fault (major fault) which can contribute to the mineralisation within those area. Based on soil profile analysis, the total REE concentration in C-horizon is higher (161.61ppm) than B-horizon (132.79ppm). However, Sc concentration is contributed the higher in C-horizon (50.37ppm) compared to B-horizon (12.35ppm).

Acknowledgment

This research is financially supported by Ministry of Higher Education Malaysia through FRGS 2021-1 (FRGS/1/2021/WAB07/UMK/02/1). Deeply acknowledgement goes to Universiti Malaysia Kelantan, UMK for providing equipment and facilities.

References

1. J. Dostal. Resources, 6(3), 34 (2017).
2. X. Feng, O. Onel, M. A. Council-Troche, A. Noble, R.-H. Yoon, & J. R. Morris. Appl Clay Sci, 201, 105920 (2021).
3. A. M. Borst, M. P. Smith, A. A Finch, G. Estrade, C. Villanova-de-Benavent, P. Nason, E Marquis, N. J. Horsburgh, K. M Goodenough, C. Xu, J. Kynický & K. Geraki. Nat Commun, 11(1) (2020).
4. Wall. Rare earth elements. Enc Geology, 680–693 (2021).
5. T.T Khoo, & B.K Tan. Technical papers, Geological Society of Thailand & Geological Society of Malaysia, 253-290 (1983).
6. E.J. Cobbing, P. E. J. Pitfield, D.P.F. Darbyshire, and D. I. J. Mallick. Brit Geol Surv, 369p (1992).
7. C. S. Hutchinson & D. N. K. Tan. *Geology of Peninsular Malaysia:*The University of Malaya and The Geological Society of Malaysia (2009).
8. Azman A. Ghani. Geol Soc Malaysia, 51, 95-101 (2005b).

9. K. R. Mohamed, N. A. Mohamed Joeharry, M. S. Leman, & C. A. Ali, C. A. Bull Geol Soc (2016).
10. A. Kontonikas-Charos, C. L. Ciobanu, & N. J. Cook. Lithos, 208-209, 178–201 (2014).
11. D. M. S. N. Dissanayake, M. M. M. G. P. G. Mantilaka, R. T De Silva, K. M. N. De Silva, & H. M. T. G. A Pitawala. Clean Mater, 1, 100016 (2021).
12. MacDonald. (1968). Geol Surv Malays Mem 10, pp 202.
13. W. F. McDonough and S, Sun. Chem Geol 120, pp. 223-253 (1995).
14. N. J. Cook, C. L. Ciobanu, K. Ehrig, A.D Slattery and S.E. Gilbert. Front. Earth Sci. 10:967189 (2022).
15. A. Kontonikas-Charos, C. L. Ciobanu, & N. J. Cook, N. J. Lithos, 208-209, 178–201 (2014).
16. M. T Aide, & C. Aide. ISRN Soil Sci, 2012, 1–11 (2012).
17. A. Jeske, & B. Gworek. Chem Spec Bioavailab, 25(3), 216–222 (2013).